Chemical Senses, 2018, Vol 43, 489–501
doi:10.1093/chemse/bjy041
Original Article
Advance Access publication 20 June 2018

Original Article

Comparison of Chemoreceptive Abilities of the Hydrothermal Shrimp *Mirocaris fortunata* and the Coastal Shrimp *Palaemon elegans*

Julia Machon[1], Philippe Lucas[2], Juliette Ravaux[1] and Magali Zbinden[1]

[1]Sorbonne Université, UPMC Univ Paris 06, MNHN, CNRS, IRD, UCBN, UAG, Unité de Biologie des organismes et écosystèmes aquatiques (BOREA, UMR 7208), Equipe Adaptations aux Milieux Extrêmes, 7 Quai Saint-Bernard, Bâtiment A, 75005 Paris, France and [2]Department of Sensory Ecology, INRA, iEES-Paris, Route de Saint-Cyr, 78026 Versailles, France

Correspondence to be sent to: Magali Zbinden, BOREA UMR7208, Sorbonne Université, Paris, France. e-mail: magali.zbinden@upmc.fr

Editorial Decision 12 June 2018.

Abstract

Chemoreception might play an important role for endemic shrimp that inhabit deep and dark hydrothermal vents to find food sources and to locate active edifices that release specific chemicals. We compared the chemosensory abilities of the hydrothermal shrimp *Mirocaris fortunata* and the coastal related species, *Palaemon elegans*. The detection of diverse ecologically relevant chemical stimuli by the antennal appendages was measured with electroantennography. The 2 species can detect food-related odor and sulfide, a short-distance stimulus, via both their antennae and antennules. Neither iron nor manganese, considered as long-distance stimuli, was detected by the antennal appendages. Investigation of the ultrastructure of aesthetasc sensilla revealed no specific features of the hydrothermal species regarding innervation by olfactory sensory neurons. Pore-like structures occurring in the aesthetasc cuticle and dense bacterial covering seem to be unique to hydrothermal species, but their potential link to chemoreception remains elusive.

Key words: aesthetasc, chemoreception, electroantennography, hydrothermal vent, sulfide

Introduction

Alvinocaridid shrimp are emblematic of deep hydrothermal vents in the Mid-Atlantic Ridge (MAR, Desbruyères et al. 2000, 2001). They inhabit patchy, ephemeral, and dark environments, depending on hot and potentially toxic fluid emissions. Several studies show that these shrimp possess a range of morphological, anatomical, and physiological adaptations to the hydrothermal environment, related to ectosymbiosis with bacteria (Casanova et al. 1993; Ponsard et al. 2013), respiration in sometimes hypoxic conditions (Lallier and Truchot 1997; Hourdez and Lallier 2007), or thermal stress (Cottin et al. 2010) for instance. However, adaptations of sensory systems have been only partially investigated (Jinks et al. 1998). Vent fauna communities are always spread around active chimneys, suggesting that they must detect attractants to choose their microhabitat, such as food sources or fluid emissions (Sarradin et al. 1999; Sarrazin et al. 1999; Le Bris et al. 2006). Among the sensory modalities that can be involved in the detection of the habitat, chemoreception might be relevant since active vents are characterized by an extensive release of various chemicals (Charlou et al. 2000). However, chemical attractants and vent shrimp chemosensory specificities are largely unknown, despite their importance for understanding how the shrimp detect their local dim environment, or new venting sites to settle in.

Considering food sources, invertebrate tissues or bacterial mats might be major attractants for scavenger species such as the hydrothermal shrimp *Mirocaris fortunata* (Gebruk et al. 2000). For the detection of hydrothermal fluid emissions, the chemicals released might be used as orientation cues. The chemical composition of fluids varies

from one site to another, but sulfide, manganese, and iron are among the compounds commonly encountered (Radford-Knoery et al. 1998; Charlou et al. 2000). Chemical gradients occur from the fluid emission point, and can be either steep or gradual depending on the chemicals (Klevenz et al. 2011). For example, around the chimneys sulfide rapidly disappears from the water column after reacting with seawater and hydrothermal fluid constituents (Mottl and McConachy 1990; Zhang and Millero 1993). Manganese is more stable (Cowen et al. 1990) and can thus be detected at considerable distances from the plume source (Radford-Knoery et al. 1998). Iron is also detected at several hundreds of kilometers from the source (Aumond 2013; Waeles et al. 2017) when partially stabilized by complexation with dissolved organic matter (Toner et al. 2009). Thus, sulfide might potentially be used by the shrimp as a short-distance stimulus, whereas manganese and iron could serve as long-distance stimuli to locate active sites to settle in during dispersion and colonization phases (Herring and Dixon 1998). Only one study gives insights into the potential role played by chemoreception in hydrothermal shrimp orientation in their environment, showing electrophysiological responses in the vent shrimp *Rimicaris exoculata* from the antenna to sulfide and preliminary behavioral observations suggesting attraction to sulfide (Renninger et al. 1995). Detection of sulfide and other fluid components must be investigated in other species to further estimate if chemicals can be used as orientation cues in vent shrimp, as well as food sources.

Chemosensory specificities can also be reflected at the anatomical level, for instance considering chemosensory sensilla fine structure. In crustaceans, the antennule is defined as the primary chemoreceptor organ (Ache 1982). Its outer flagellum carries specialized unimodal olfactory sensilla called aesthetascs, innervated by many bipolar olfactory sensory neurons (OSNs, Laverack 1964; Grünert and Ache 1988; Hallberg et al. 1992; Derby and Weissburg 2014). Dendrites of OSNs from various decapod crustaceans exhibit a similar ultrastructure (Ghiradella et al. 1968), with inner dendritic segments (IDSs) that emanate from the cell bodies and divide into the aesthetasc shaft in outer dendritic segments (ODSs) that bear the chemoreceptors (Grünert and Ache 1988). Aesthetascs are also characterized by the absence of a terminal pore, resulting in a necessarily thin cuticle to allow the passing of soluble odorant molecules that must bind their cognate receptors located on the dendritic membranes of the OSNs (Blaustein et al. 1993; Derby et al. 2016). The fine structure of aesthetascs of large decapods such as lobsters or crayfishes has been extensively described (Altner and Prillinger 1980; Ache 1982; Derby 1982; Laverack 1988; Hallberg and Chaigneau 2004), and show that variations occur in the cuticle thickness and the number of IDSs and ODSs. Determination of these parameters for hydrothermal shrimp could reveal potential links to chemoreception efficiency or adaptation to the environment. A second mode of chemoreception is called distributed chemoreception and is mediated by bimodal sensilla (Cate and Derby 2001; Schmidt and Mellon 2010) innervated by mechano- and chemosensory neurons (Schmidt and Ache 1996) and located mainly on antennular and antennal appendages, mouthparts, chelipeds, and walking appendages (Ache 1982; Garm et al. 2003; Garm and Walting 2013). They are characterized by a densely arranged cuticle and display a terminal or subterminal pore (Garm et al. 2003). Bimodal sensilla are usually considered as short-range or contact chemosensory sensilla, whereas unimodal aesthetascs mediate distant detection of chemicals, referring to olfaction (Hallberg and Skog 2010; Schmidt and Mellon 2010).

We conducted a comparative study on the vent shrimp *M. fortunata* and the coastal shrimp *P. elegans* to identify possible chemosensory adaptations of endemic vent shrimp compared to a shallow water species, as well as potential chemical attractants for the hydrothermal species. Chemical senses are susceptible to evolve rapidly (Bargmann 2006) and those of crustaceans present specialized adaptations that can vary with their phylogeny, lifestyle, and trophic level (Derby and Weissburg 2014). Adaptations can be related to differences in sensitivity to feeding and orientation cues (Fuzessery and Childress 1975), or to anatomical modifications of chemosensory organs, such as the number of OSNs innervating each aesthetasc (Ghiradella et al. 1968). To test whether the 2 shrimp species are able to detect common food sources (such as dead shrimp extract) and hydrothermal fluid components (such as sulfide, manganese, and iron) through their presumed main chemosensory organs, we used an electroantennography (EAG) method that we recently developed for shrimp (Machon et al. 2016) to record the global response of the antennal appendage neurons to environmental stimuli. We also compared between the 2 species the number of IDSs and ODSs innervating each aesthetasc with transmission electron microscopy (TEM), to see if the vent shrimp presents anatomical differences that could potentially indicate an enhanced chemosensitivity. The structure of the aesthetasc cuticle was also investigated because it determines the access of odorants to their chemoreceptors. This combined functional and anatomical approach aims to enhance the general knowledge on shrimp chemoreception, and ultimately to provide insights into the potential adaptations of hydrothermal shrimp chemosensory system to detect their particular environment.

Materials and methods

Animal collection, conditioning, and maintenance

Specimens of Alvinocaridid shrimp *M. fortunata* (Martin and Christiansen 1995) used for histology were collected on the Lucky Strike vent site (MAR, 37°17'N, 1700 m depth) during the Momarsat 2011 and 2012 cruises and on the Menez Gwen vent site (MAR, 37°50'N, 850 m depth) during the Biobaz 2013 cruise. Samples used for electrophysiological experiments were collected on the Lucky Strike vent site during the Momarsat 2016 cruise. Shrimp were sampled with the suction sampler of the Remotely Operated Vehicle "Victor 6000" operating from the research vessel "Pourquoi pas?". Immediately after recovery, specimens for histology and ultrastructure observations were dissected and tissues of interest were fixed in 2.5% glutaraldehyde/seawater solution (see below) and kept in seawater/NaN_3 rinsing solution until use at laboratory. Specimens for EAG were acclimated to atmospheric pressure in tanks of approximately 5–10 L of seawater at a temperature of 5–9 °C. At the end of the cruise, shrimp were transferred to the Oceanopolis aquarium in Brest, France, and recovered from the sampling during 2 weeks before transfer to the laboratory. There, 40 shrimp were housed communally in a 100 L aquarium with oxygenated artificial seawater (Red Sea Salt, Red Sea, Houston, TX, USA) at 8 ± 1 °C under natural light:dark cycle, and fed twice a week with shrimp food powder (Liptoaqua, Madrid, Spain). In both locations, aquaria had a 50 W thermostat heater set to 25 °C to serve as a hot spot for the shrimp.

Caridean shallow water shrimp *P. elegans* (Rathke 1837) were collected from Saint-Malo Bay, France, in October 2016 using a shrimp hand net. They were housed communally as for *M. fortunata*, at room temperature (20 ± 1 °C), without heater, and fed 3 times a week with shrimp food pellets (Novo Prawn, JBL, Neuhofen, Germany).

Electroantennography

EAG recordings were performed as previously described (Machon et al. 2016). Electrodes were pulled from GB150F-8P glass capillaries (Science Products, Hofheim, Germany) using a P-97 puller (Sutter Instrument, Novato, CA). They had a tip diameter of 1 to 2.5 µm and

were filled with *Panulirus* saline (PS, composition in chemical stimuli). The reference electrode was introduced through the soft articular membrane between the telson and the abdomen. The recording electrode was inserted with a NMN-25 micromanipulator (Narishige, London, United Kingdom) in the middle region of the flagellum area bearing the aesthetascs, between 2 aesthetasc rows, for the lateral flagellum of the antennule (referred as "antennule" further in the text), and between 2 annuli of the proximal region (first quarter) for the antenna. Signals were amplified (×100) and filtered (0.1–1000 Hz) using an EX1 amplifier with a 4002 headstage (Dagan, Minneapolis, MN), and digitized at 2 kHz by a 16-bit acquisition board (Digidata 1440A) under Clampex 10.3 (Molecular Devices, Sunnyvale, CA). Data were analyzed using Clampfit (Molecular Devices). Signals were low-pass filtered offline at 20 Hz.

A gravity-fed PS perfusion was positioned over the branchial cavity to maintain the shrimp alive. For *M. fortunata*, the PS perfusion was maintained at 9 ± 1 °C using ice packs. Chemical stimuli were delivered by a pressurized perfusion system with 8 channels (AutoMate scientific, Berkeley, CA). To prevent oxidation of the iron, manganese, and sulfide solutions within reservoirs, the system was pressurized under nitrogen gas. Reservoirs were connected to a segment (70 mm) of deactivated gas chromatography (GC) column (0.25 mm internal diameter). The tip of the GC column was positioned with a UM-3C micromanipulator at ~1 mm from the recorded flagellum, and ~45° from its longitudinal axis.

Stimuli were applied for 1 s at 5 psi (1.1 $mL.min^{-1}$). Consecutive stimuli were delivered with at least 90 s intervals to prevent chemosensory adaptation (Machon et al. 2016). In addition to continuous renewing of the PS bath solution with a gravity-fed perfusion, half of the medium was replaced after applying each stimulus with new PS using a 10 mL syringe. Between stimuli, the dead volume of the stimulus device (GC column) was rinsed outside of the Petri dish, first with PS and then with the solution of the next stimulus. To establish the dose–response relationship for each stimulus, stimuli were applied in increasing concentrations, always starting with the negative control (PS). Responses to the positive control (aqueous extract of shrimp food, see below) were applied at the end of the experiment to ensure the recording quality. Recordings of low quality were excluded from the analysis by discarding experiments for which the amplitudes of responses to the positive control were smaller than 0.3 and 0.08 mV for the antennule and the antenna, respectively. When responses to the negative control had different amplitudes at the beginning and at the end of an experiment, the average of the 2 values was used.

Chemical stimuli

PS was used to prepare all stimuli and as a negative control. The composition of PS was (in $mmol.L^{-1}$) 486 NaCl, 5 KCl, 13.6 $CaCl_2$, 9.8 $MgCl_2$, and 10 HEPES, pH: 7.8–7.9 (Hamilton and Ache 1983), with osmolarity adjusted to 1050 mOsm/L with mannitol.

An aqueous extract of shrimp Novo Prawn food pellets (NP) was used as positive control in all experiments. Food pellets were dissolved for 48 h at room temperature at 0.2 $g.mL^{-1}$ in PS. The extract was then centrifuged at 5900 g for 10, 15, and 20 min and the supernatant was collected after each centrifugation and filtered (0.45 µm), aliquoted and stored at –20 °C until use.

Aqueous extracts of dead *M. fortunata* and dead *P. elegans* individuals were prepared in PS from material kept for 48 h at room temperature at approximately 75 $mg.mL^{-1}$. Extracts were then centrifuged at 2000 g with a Galaxy MiniStar microcentrifuge and the supernatant was filtered (0.45 µm), aliquoted and stored at –20 °C. Before use, pH was adjusted to 7.8–7.9 and solutions were diluted 10 and 100 times.

For stimuli characteristic of hydrothermal fluids (sulfide, iron, and manganese), dose–response relationships were established with concentrations in the range of those that *M. fortunata* is likely to encounter its environment (sulfide, 2–20 $µmol.L^{-1}$; iron, 0.2–2.5 $µmol.L^{-1}$ [Sarrazin et al. 2015]; manganese, 0.004–4.8 $µmol.L^{-1}$ [Aumond 2013]) to concentrations in the range of those of the hydrothermal fluid at the Lucky Strike vent site (sulfide, 2–15 $mmol.L^{-1}$ [Renninger et al. 1995]; iron, 30–863 $µmol.L^{-1}$; manganese, 50–450 $µmol.L^{-1}$ [Charlou et al. 2000]). To minimize oxidation, all solutions were prepared under a funnel connected to a nitrogen gas bottle, with PS previously deoxygenated by bubbling nitrogen for 5–10 min. All dilutions were made the day of use. Stimuli, concentrations, and controls used for EAG are given in Table 1.

In order to simulate the concentrations that *M. fortunata* encounters in its environment, stock solutions were prepared at 2 $mmol.L^{-1}$ in deoxygenated PS, with pH adjusted to 2 for $FeCl_2$ (reference 372870, Sigma-Aldrich) and $MnCl_2$ (reference M8054, Sigma-Aldrich) solutions, and to 9 for Na_2S (reference 208043, Sigma-Aldrich) solution. Stock solutions were diluted with deoxygenated PS. The concentrations 40 $µmol.L^{-1}$ for Na_2S and 5 $µmol.L^{-1}$ for $FeCl_2$ and $MnCl_2$ correspond to the estimated concentrations in the environment of *M. fortunata* (Sarrazin et al. 2015 for iron and sulfide, Aumond 2013 for manganese). For higher concentrations, 4 concentrations were chosen on a logarithmic scale, the lowest corresponding to the estimated concentration in the environment of *M. fortunata*, and the second highest corresponding to the concentration measured in the pure fluid at the Lucky Strike vent site (Charlou et al. 2000). Solutions were prepared in deoxygenated PS with serial dilutions from the highest concentration. For $FeCl_2$ solutions, pH was adjusted to 6 to avoid iron precipitation. PS adjusted to pH 6 was used as a pH control for $FeCl_2$ stimulation series, and PS adjusted to pH 11 was used as a pH control for Na_2S stimulation series, to match the pH of the highest concentrated Na_2S solution (14 $mmol.L^{-1}$).

Statistical analysis

For EAG data, 1-way ANOVA with permutation test was used to test differences among amplitudes of EAG responses to concentrations of each stimulus. For significant results, 2-sided 2-sample permutation test using Welsh's t test was performed to investigate the difference with the negative control for each concentration. Data are given as means (standard deviation [SD]).

Data analyses were carried out using RStudio v.1.0.136 software.

Transmission electron microscopy

For anatomical observations, lateral flagella of the antennules were used. Tissues were postfixed in osmium tetroxide 1%, dehydrated in ethanol and propylene oxide series, and further embedded in epoxy resin (Agar Scientific). Ultrathin sections were made from the middle region of lateral flagella on a Leica Ultramicrotome (Ultracut R) using a diamond knife, and were laid on 150 or 200-mesh copper grids and stained with saturated solution of uranyl acetate at 60 °C. Observations were carried out on a Hitachi H7100 transmission electron microscope operating at 75 kV.

Ultrastructural analysis

Anatomical traits of the aesthetascs, the cuticle thickness and the number of inner and outer dendritic segments (respectively IDSs and ODSs; Figure 1), were estimated from TEM observations, using ImageJ software. Measurements of cuticle thickness were made on sections at various levels of 20 and 30 aesthetascs for *M. fortunata* (5 individuals)

Table 1. Solutions and number (*n*) of antennules and antennae tested for each condition in EAG

Stimulus	Concentrations, dilutions, controls	*N*			
		Antennules		Antennae	
		Mirocaris fortunata	*Palaemon elegans*	*Mirocaris fortunata*	*Palaemon elegans*
Figure 2					
Shrimp food extract	0.2 g.mL^{-1}	44	58	13	27
PS	—				
Dead shrimp extract	Non-diluted; 1:10; 1:100	7	8	—	—
Figure 3					
Na_2S	PS (negative control)	9	12	4	8
	PS pH 11 (pH control)	4	7	4	8
	0.04, 0.1, 0.4, 1, 4 µmol.L^{-1}	5	5	—	—
	40 µmol.L^{-1}	8	12	4	8
	300, 2000, 14 000 µmol.L^{-1}	4	7	4	8
$FeCl_2$	PS (negative control)	11	15	5	9
	PS pH 6 (pH control)	6	10	5	9
	0.05, 0.1, 0.5, 1 µmol.L^{-1}	5	5	—	—
	5 µmol.L^{-1}	10	15	5	9
	60, 900, 10 000 µmol.L^{-1}	6	10	5	9
$MnCl_2$	PS (negative control)	10	17	4	10
	0.05, 0.1, 0.5, 1 µmol.L^{-1}	5	6	—	—
	5 µmol.L^{-1}	9	17	4	10
	50, 500, 3500 µmol.L^{-1}	5	11	4	10

and *P. elegans* (4 individuals), respectively. Data for cuticle thickness are given as minimum and maximum values. The number of IDSs per aesthetasc was estimated from counts in several 25 to 150 µm^2 portions of sections from the base of the sensilla, on 11 and 13 aesthetascs for *M. fortunata* (3 individuals) and *P. elegans* (2 individuals), respectively. The number of ODSs per aesthetasc was estimated from counts in several 4 to 30 µm^2 portions of the sensilla judged to contain the highest number of ODSs containing single microtubules, on 7 and 28 aesthetascs for *M. fortunata* (4 individuals) and *P. elegans* (4 individuals), respectively. Data for IDS and ODS are given as range.

Results

EAG responses to chemicals

Stimulations of the antennal appendages with a shrimp food extract (NP, positive control) always triggered positive deviations of the baseline (Figure 2A). Antennular responses to NP extract had a significantly higher amplitude in *P. elegans* than in *M. fortunata*. By contrast, the amplitude of antennal responses to the NP extract were significantly higher in *M. fortunata* than in *P. elegans*. Responses to the negative control (PS) were always negative deviations of the baseline for the antennule, but were either positive or negative for the antenna (Figure 2B). Responses to PS from the antenna were much lower than responses from the antennule for both species.

Responses of the antennule to dead shrimp extracts were dose-dependent (Figure 2C), with a threshold dilutions between 1:100 and 1:10 for *P. elegans*, and between 1:10 and non-diluted for *M. fortunata*, and amplitudes reaching 250 and 70 µV for the nondiluted extract for *P. elegans* and *M. fortunata*, respectively.

At concentrations of *M. fortunata* environment, for the stimuli tested (Na_2S: 0.04–40 µmol.L^{-1}; $FeCl_2$ and $MnCl_2$: 0.05–5 µmol.L^{-1}) responses from the antennule of *M. fortunata* and *P. elegans* did not depend on stimulus concentrations (Figure 3A,C,E, white bars).

At higher concentrations, Na_2S elicited dose-dependent responses from both the antennules and antennae of *M. fortunata* and *P. elegans* (Figures 3A,B and 4). Thresholds were between 0.3 and 2 mmol.L^{-1} for the antennules of both species and for the antennae of *M. fortunata*, and between 2 and 14 mmol.L^{-1} for the antennae of *P. elegans*. For *M. fortunata*, amplitudes for the highest concentration (14 mmol.L^{-1}) reached 120 µV for the antennule and 50 µV for the antenna. For *P. elegans*, they reached 20 µV for the antennule and 110 µV for the antenna. Increasing concentration of $FeCl_2$ (0.005–10 mmol.L^{-1}) and $MnCl_2$ (0.005–3.5 mmol.L^{-1}) solutions did not trigger dose-dependent responses from the antennules and the antennae (Figure 3C,D,E,F) for both species.

pH control solutions were used to distinguish responses triggered by the chemicals or by the pH of the solutions (pH 11 for Na_2S 14 mmol.L^{-1}, and pH 6 for all high concentration $FeCl_2$ solutions). Mean response of *P. elegans* antennae to pH control solution (pH: 11) significantly differed from the negative control (PS) and from the response to the highest Na_2S concentration (14 mmol.L^{-1}) (Figure 3B). This pH control solution did not trigger response different from the negative control (PS) for the antenna of *M. fortunata*, and for the antennules of the 2 species (Figure 3A,B). The pH control solution for high concentration $FeCl_2$ series (pH 6) did not elicit any significant response for both antennae and antennules for the 2 species (Figure 3C,D).

Aesthetascs cuticle and innervation

The thickness and ultrastructure of the cuticle of aesthetascs vary over the length of the sensilla (Table 2). From the base to the transitional zone (see Figure 1), the aesthetasc cuticle is thick for the 2 species, from 0.8 to 1.8 µm (minimum and maximum values) in *M. fortunata* and from 0.6 to 1.3 µm in *P. elegans*. Just distal to the transitional zone, in *P. elegans* the cuticle becomes thin (0.6–0.3 µm) on almost all the distal part of the sensilla (80% of the length), with the cuticle at the tip of the aesthetasc thinning to 0.15 µm. In

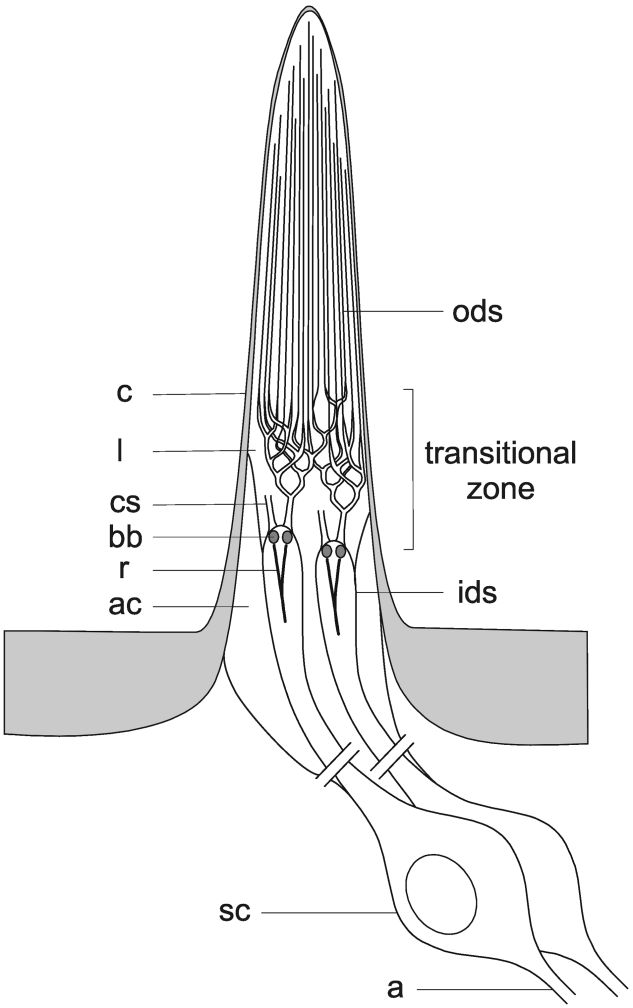

Figure 1. Schematic representation of an aesthetasc from a marine crustacean decapod. Only 2 of approximately 100–400 bipolar olfactory sensory neurons that innervate each aesthetasc are shown, and for each neuron only 1 cilium branching is shown. The transitional zone refers to the zone where the inner dendritic segments give rise to 2 ciliary segments, each starting to divide dichotomously in outer dendritic segments. Axon (a); accessory cell (ac); basal bodies (bb); cuticle (c); ciliary segment (cs); inner dendritic segment (ids); outer dendritic segment (ods); ciliary rootlet (r); lumen (l); sensory cell somata (sc). Not to scale.

M. fortunata the cuticle remains thick on the first half of the aesthetasc length, and becomes thin on the distal half of the sensilla, from 0.8 to 0.15 µm. For each species, the thick cuticle has a lamellar structure (Figure 5A,B), which gradually becomes loose when thinning (Figure 5C,D). In *M. fortunata*, pore-like structures occur in the lamellar cuticle (Figures 5A,E and 6C). They can reach approximately 0.2 µm in diameter, open to the inner side of the aesthetasc and are separated from the outside by a cuticle layer that thins from 0.4 to 0.06 µm. They are present from the transitional zone to approximately 50 % of the aesthetasc length, when the cuticle starts to thin, and are no longer present in the loose part of the cuticle (Figure 5C). These pore-like structures were also observed in the same region of the aesthetascs in the hydrothermal shrimp *R. exoculata* (Figure 5F), with a diameter slightly larger (up to 0.4 µm). For these 2 hydrothermal species, the aesthetascs are often covered by bacteria (Figure 5C,E,F) over their entire length. Neither pore-like structures, nor bacteria have ever been observed in *P. elegans*.

A schematic view of the dendrites regionalization (with IDSs, ODSs, and transitional zone) within an aesthetasc is presented in Figure 1. IDSs are surrounded by auxiliary cells (Figure 6B) and extend into the lumen of the aesthetasc, where they terminate at various levels within the transitional zone. They contain mitochondria, microtubules, vesicles, and a ciliary rootlet (Figure 6A,B). Each aesthetasc contains approximately 90 to 223 IDSs for *M. fortunata* and 177 to 519 IDSs for *P. elegans*, meaning each aesthetasc is innervated by approximately 90 to 223 and 177 to 519 OSNs for *M. fortunata* and *P. elegans*, respectively (Table 2). ODSs are not surrounded by auxiliary cells, the remaining area is filled with lymph (Figure 6C,D). Swellings occur along the entire length of the outer dendritic segments (Figure 6C,D). There is approximately 2545 to 5383 and 1568 to 10637 ODSs per aesthetasc for *M. fortunata* and *P. elegans*, respectively (Table 2).

Discussion

Detection of food-related odor mixtures

M. fortunata exhibits an opportunistic feeding behavior, scavenging on tissues of mussel, shrimp, and other invertebrates when available, as well as grazing bacteria on sulfide surfaces (Gebruk et al. 2000; Colaço et al. 2002; De Busserolles et al. 2009). We used an extract of dead *M. fortunata* as an environmental relevant food-odor stimulus to test whether the detection of food is mediated by the antennule for this species. This stimulus elicited dose-dependent responses from the antennule, confirming its presumed role in food detection. An extract of dead *P. elegans* also stimulated the antennule of *P. elegans*. These results are consistent since *P. elegans* and *M. fortunata* have a similar food profile, being secondary consumers. EAG responses to positive control (NP), from both the antennule and the antenna, suggest that the antenna is also involved in the chemodetection of food sources in both species. The detection of food sources by the antennal appendages of *M. fortunata* indicates that this hydrothermal species may rely on food-related odors to detect its habitat as can do coastal species, but the influence of food stimuli in maintaining shrimp around vent chimneys need to be further investigated with behavioral experiments.

Detection of hydrothermal fluid stimuli

Chemicals and their concentrations were chosen regarding the chemical composition of the hydrothermal fluids (Radford-Knoery et al. 1998; Charlou et al. 2000) and in the shrimp vicinity (Aumond 2013; Sarrazin et al. 2015) at the Lucky Strike hydrothermal vent site, where *M. fortunata* specimens were sampled. Each chemical presents different removal rates, associated to reaction with seawater, other hydrothermal fluid constituents, dissolved organic matter, and to consumption by chemoautotrophic bacteria. Sulfide removal rate is high and sulfide is thus considered as a short-distance stimulus, detectable near hydrothermal fluid emission points, whereas manganese and iron are more stable, detectable far from the source, thus are considered as long-distance stimuli (Radford-Knoery et al. 1998; Aumond 2013; Waeles et al. 2017). To investigate if vent shrimp use such hydrothermal fluid compounds as orientation cues for both near-field and distant perception of the habitat, we tested the detection of selected chemicals by the antennular and antennal appendages of *M. fortunata*, as well as those of the coastal shrimp *P. elegans*, to check for potential hydrothermal shrimp specificity. Each chemical was first tested on the antennules at concentrations that *M. fortunata* is likely to encounter in its environment, but none elicited responses distinct from responses to the negative control.

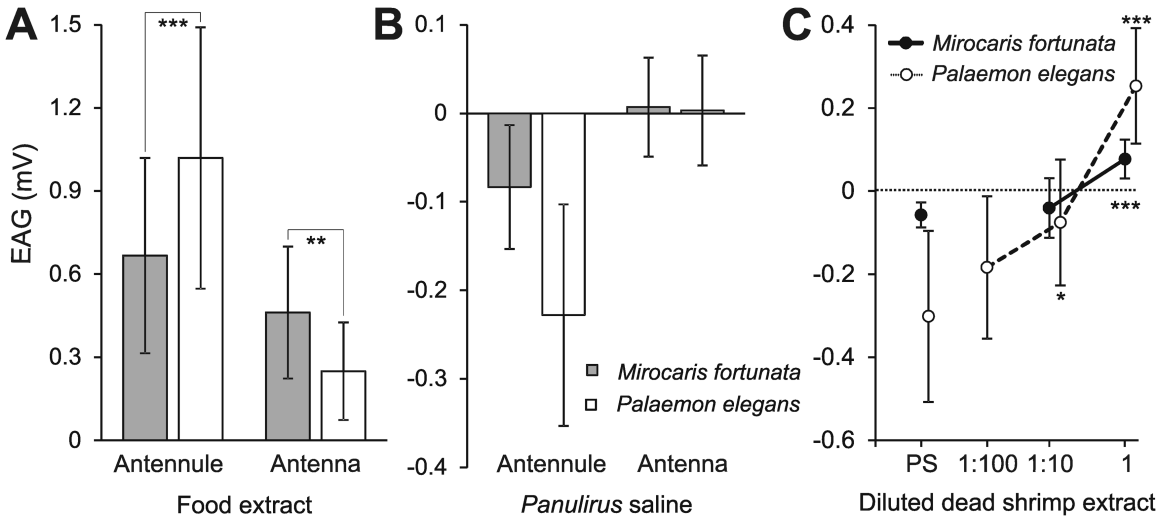

Figure 2. EAG responses to food extract stimulus, to negative control, and to dead shrimp extracts. Responses to (A) a shrimp food extract 0.2 g.mL^{-1} and to (B) PS (negative control) recorded from the antennules and antennae (gray, *Mirocaris fortunata*; white, *Palaemon elegans*), and to (C) dead shrimp extracts recorded from the antennules. For (A) and (B), means (SD) were compared between 2 species for each organ and stimulus with a 2-sample permutation *t*-test. For (C), means (SD) were compared with a 1-way ANOVA with permutation test ($P < 10^{-15}$) and with a 2-sample permutation *t*-test to control stimuli (PS). $^{**}P < 0.01$, $^{***}P < 0.005$. The *n* numbers of antennules and antennae tested for each species and for each condition are presented in Table 1.

We then used high concentrations, up and beyond to the concentrations measured in the pure fluid of the Lucky Strike vent site, on the antennule and antenna of both species. Sulfide elicited responses in a concentration-dependent manner for both the antennules and the antennae in *M. fortunata*. Thus sulfide is detected by bimodal sensilla from the antennae, but for the antennules we cannot distinguish the role played by aesthetascs and bimodal sensilla in sulfide detection. Renninger et al. (1995) recorded trains of action potentials from nerve fibers of the 3 antennal appendages of the hydrothermal shrimp *R. exoculata*, and found that only the antennae respond in a graded way to sulfide. This absence of concentration-dependent responses for the antennule in *R. exoculata* might be due to technical limitations rather than no detection. Recording from nerve fibers implies that only a fraction of axons are connected to the electrode opening, and thus action potentials are recorded from only a minority of neurons. The EAG method overcomes this problem since the electrode records neuron activation from almost the whole length of the flagellum (Machon et al. 2016). Hence at least 2 hydrothermal shrimp species are physiologically able to detect sulfide via their antennal appendages, supporting the hypothesis that sulfide could serve as an effective orientation cue at short distance of the hydrothermal vent. Yet because the sulfide concentrations that triggered significant EAG responses were equivalent to those encountered in the pure fluid, there is some doubt about the ecological relevance of the responses obtained since *M. fortunata* inhabits diffuse vents with low chemical concentrations (Cuvelier et al. 2011), and *R. exoculata* lives closer to vent chimneys but still in fluid-diluted areas. However, convergence of sensory inputs onto higher-level neurons occurs in the chemosensory pathway of crustaceans (Mellon 2000), as in vertebrates and insects (Van Drongelen et al. 1978). This convergence makes second-order neurons in the central nervous system more sensitive than peripheral chemosensory neurons (Rospars et al. 2014). Hence, behavioral responses to chemical stimuli can potentially be observed at concentrations that do no trigger EAG responses, and questions regarding the relevance of the sulfide concentrations tested could be addressed with behavior experiments. Antennules and antennae of the coastal shrimp *P. elegans* were also responsive to sulfide in this study, meaning that sulfide detection is not specific to vent species and is likely not an adaptation to the hydrothermal environment. Again, behavior experiments are needed to investigate if hydrothermal species present specific responses to sulfide, such as attraction behavior, compared to coastal species.

P. elegans antenna was also significantly responsive to a control pH 11 stimulus, as observed by Renninger et al. (1995) for the coastal shrimp *Palaemonetes aztecus* antenna exposed to a pH 13 stimulus. But the response to pH 13 in *P. aztecus* was not significantly different from the response to a pH 13 sulfide solution (1300 mmol.L^{-1}). In this study, response of the antenna in *P. elegans* to pH 11 significantly differs in amplitude from the response to pH 11 sulfide solution (Na_2S 14 mmol.L^{-1}), meaning there is detection of both sulfide and high pH by the antenna of *P. elegans*. The confounded responses to sulfide and pH 13 stimulus in *P. aztecus* (Renninger et al. 1995) might be due to the low number of specimens tested ($1 < n < 4$), insufficient to bring out a significant difference between these 2 stimuli. Responses to high pH stimuli could be specific to coastal species, because neither *M. fortunata* antenna (this study) nor *R. exoculata* antenna (Renninger et al. 1995) were significantly responsive to basic pH solutions. However, in shallow habitats extreme pH are rarely encountered and may appear as ecologically irrelevant stimuli that should not evoke any behavioral response (Puri and Faulkes 2010). Note that pH 11 stimulus was used in this study as a control for the highest concentrated sulfide solution, not as a pH stimulus. To investigate the detection of pH variations as an orientation cue for hydrothermal shrimp, acid pH solutions should be tested because in Lucky Strike hydrothermal fluid pH ranges from 3.84 to 6.45 (Charlou et al. 2000), and from 6.1 to 7.3 in the shrimp habitat (Desbruyères et al. 2001).

Detection of manganese and iron by a vent shrimp was tested here for the first time, and the 2 stimuli did not trigger responses at any concentration tested. This suggests but does not definitely proves that shrimp cannot detect these compounds since the sensitivity of the EAG method is limited. EAG represents the summation of receptor potentials generated by many sensory neurons responding simultaneously (Nagai 1985). Thus, if iron and manganese stimulate only a low number of chemosensory neurons, the sensitivity of the EAG

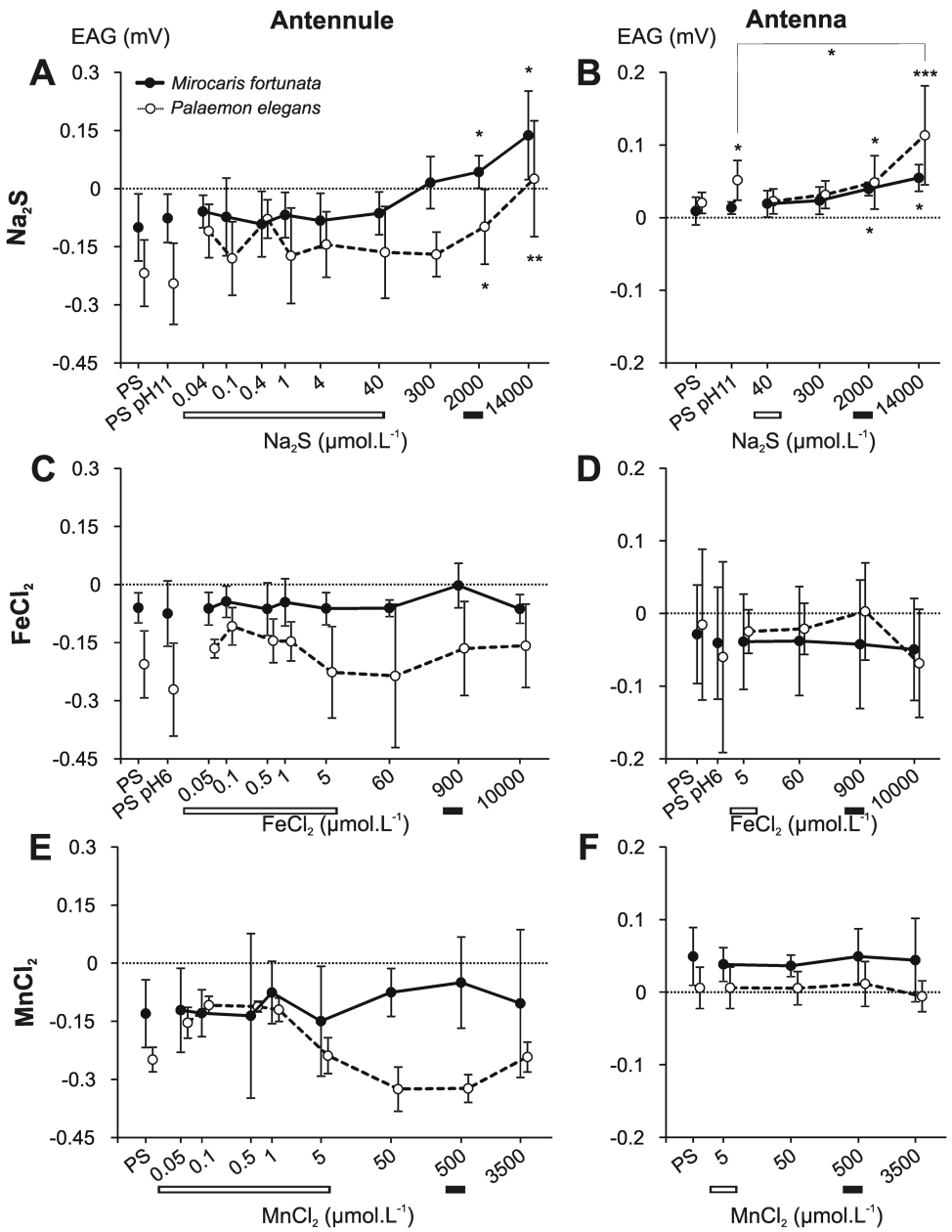

Figure 3. EAG responses from the antennules and the antennae to hydrothermal fluid compounds. EAG responses to increasing concentrations for Na_2S, $FeCl_2$, and $MnCl_2$ in *Mirocaris fortunata* (black dots) and *Palaemon elegans* (white dots). (A) Responses to Na_2S recorded from the antennules. (B) Responses to Na_2S recorded from the antennae. For (A) and (B), pH control is set to 11 and corresponds to the pH of the 14 000 µmol.L^{-1} Na_2S solution. (C) Responses to $FeCl_2$ recorded from the antennules. (D) Responses to $FeCl_2$ recorded from the antennae. For (C) and (D) pH control is set to 6 and corresponds to the pH of the 5–10000 µmol.L^{-1} $FeCl_2$ solutions. (E) Responses to $MnCl_2$ recorded from the antennules. (F) Responses to $MnCl_2$ recorded from the antennae. Under the *x* axis, white bars indicate concentrations that *M. fortunata* is likely to encounter in its environment, and black bars indicate concentrations measured in the pure fluid at the Lucky Strike vent field. Means (SD) were compared with a 1-way ANOVA with permutation test ($P < 10^{-15}$ for sodium sulfide dose-responses) and with a 2-sample permutation *t*-test to control stimuli (PS). *$P < 0.05$, **$P < 0.01$, ***$P < 0.001$. The *n* numbers of antennules and antennae tested for each species and for each condition are presented in Table 1.

method is most likely not sufficient to detect a response. However, the alternative that manganese and iron are actually not detectable by vent shrimp raises questioning about the relative importance of chemoreception for these animals. Manganese and iron are relevant stimuli for long-distance detection of hydrothermal fluids, which is a fundamental issue regarding vent shrimp lifestyle. Because hydrothermal vents are dynamic and ephemeral ecosystems, vent animals need to detect new venting sites to settle in, and the extremely high abundances of shrimp on MAR sites (Polz et al. 1998; Martin and Haney 2005) suggest that they are successful colonizers. Which fluid attractants are used for the long-distance detection of active sites, in addition to which stage of life are involved (Herring and Dixon 1998; Tyler and Young 2003), is still uncertain. Since sulfide, although emblematic of vent chemicals, is not a relevant stimulus in this context, the prospective that vent shrimp cannot detect manganese and iron makes the distant chemodetection of hydrothermal

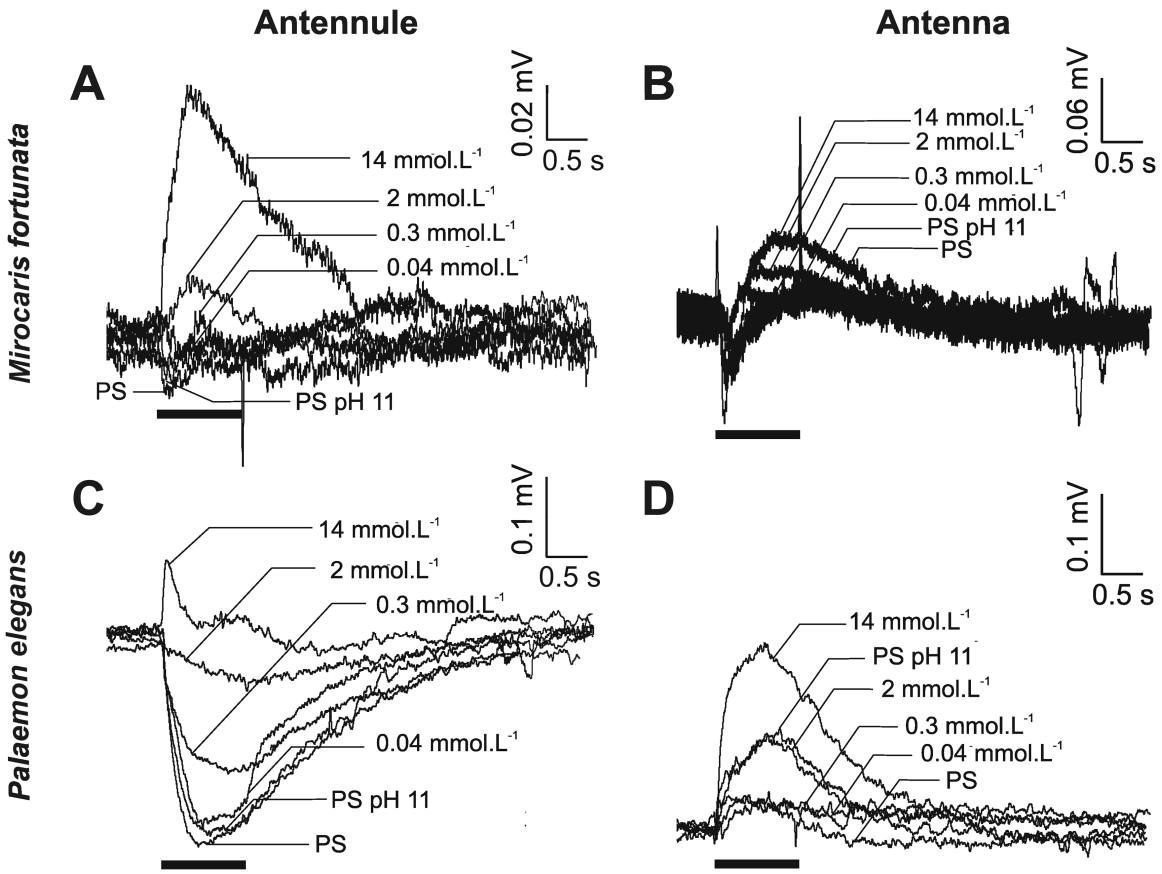

Figure 4. Dose-dependent EAG responses to Na_2S solution from the antennule and the antenna of the 2 shrimps. Superimposed traces of EAG responses to PS, to increasing concentrations of Na_2S (0.04, 0.3, 2, 14 mmol.L^{-1}) and to pH control solution (PS at pH 11) from the antennule (A, C) and the antenna (B, D) in *Mirocaris fortunata* (A, B) and *Palaemon elegans* (C, D). Horizontal bars indicate stimulus delivery. Transient peaks in A, B, and D are valve opening artifacts.

Table 2. Comparison of cuticle thickness and number of IDSs and ODSs in aesthetascs of marine crustacean decapod species

Species	Thickness of "thick" cuticle (µm)	Thickness of "thin" cuticle (µm)	Number of IDSs per aesthetasc[a]	Number of ODSs per aesthetasc[a]	References
Marine crab					
Cancer productus	2.1	1.1	100	—	Ghiradella et al. 1968
Callinectes sapidus	—	—	105	1420	Gleeson et al. 1996
Marine hermit crab					
Pagurus hirsutiusculus	1.3	0.4	400	6000–8000	Ghiradella et al. 1968
Spiny lobster					
Panulirus interruptus	4	1	300	—	Spencer and Linberg 1986
Panulirus argus	3	0.8	300–350	8000–10 000	Grünert and Ache 1988
Caridean shrimp					
Palaemon adspersus	1	0.4	—	—	Solari et al. 2017
Palaemon elegans	1.3	0.14	177–519	1568–10 637	This study
Mirocaris fortunata	1.5	0.15	90–223	2545–5383	This study

[a]Estimations presented as range.

plume doubtful. Detection of other long-distance relevant chemicals such as methane (de Angelis et al. 1993) should be tested, as well as other possible long-distance attractants such as noise (Crone et al. 2006) or temperature (Baker et al. 2016). Chemoreception abilities of other life stages should also be investigated, although larval dispersal is thought to play a role in colonization processes (Lutz et al. 1984) and aesthetasc sensilla are present in Alvinocaridid first zoeal stages (Hernandez-Avila et al. 2015).

Comparison of aesthetasc cuticle and innervation

Differences in chemosensitivity between 2 species, as specific adaptations to a particular environment, may be reflected by anatomical dissimilarities (Beltz et al. 2003). Although the general organization of aesthetascs and OSNs is analogous between decapod species (Ghiradella et al. 1968), the aesthetasc cuticle thickness and the numbers of IDSs and ODSs can vary. The cuticle thickness relates to the permeability of the aesthetasc, thus the ability to detect

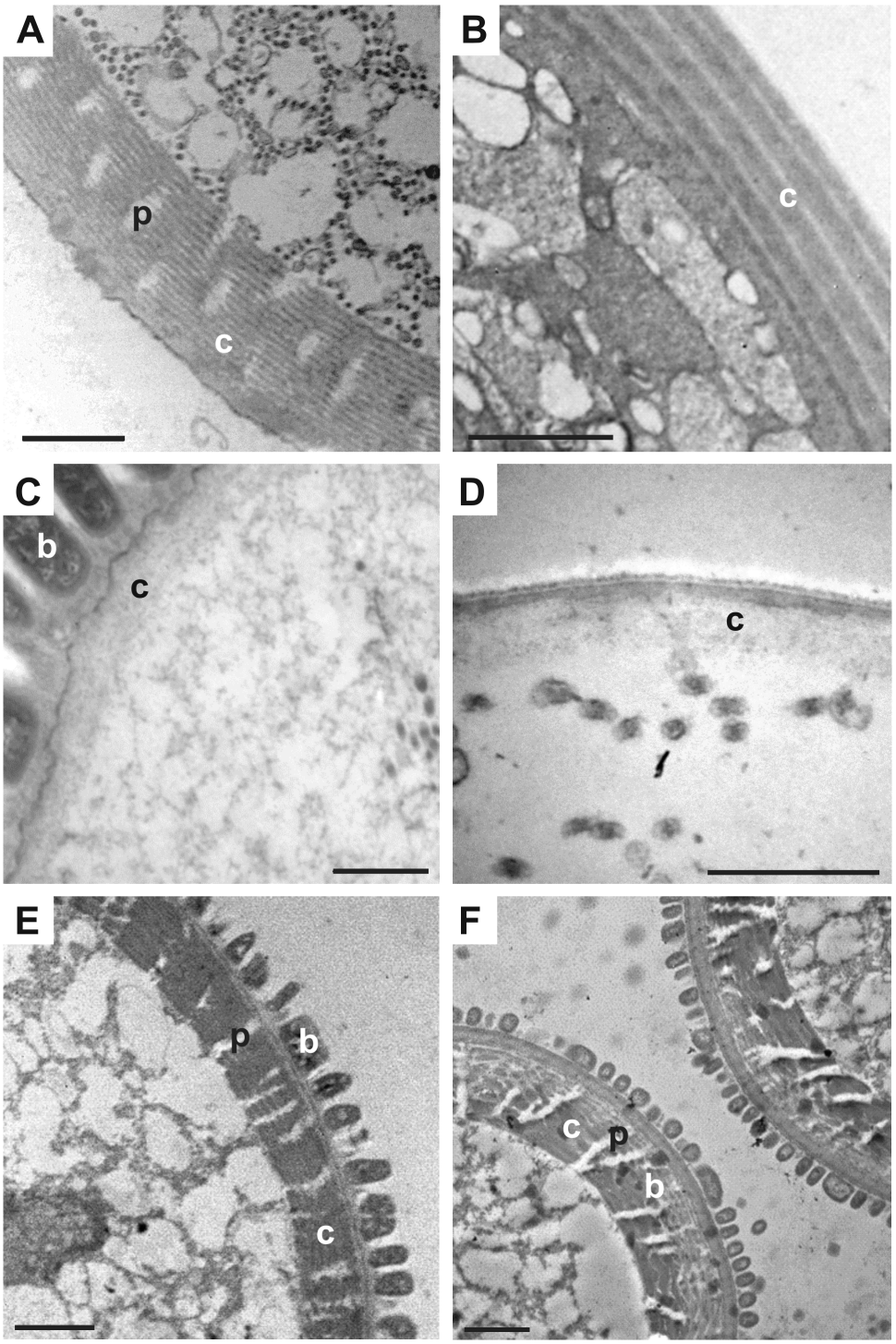

Figure 5. Cuticle of aesthetasc sensilla of *Mirocaris fortunata* (A, C, E), *Palaemon elegans* (B, D), and *Rimicaris exoculata* (F). Cross sections through the base (B), the middle (A, E, F), and the apex region (C, D) of the aesthetascs. Bacterium (b); cuticle (c); pore-like structure (p). Scale bar = 1 µm.

soluble odorants. IDSs and ODSs refer respectively to the number of OSNs and dendrites innervating the aesthetasc, and could be linked to odorant discrimination ability (Derby and Weissburg 2014). Aesthetasc ultrastructure has been well described for several decapod models (Table 2; Laverack and Ardill 1965; Ghiradella et al. 1968; Snow 1973; Hallberg and Chaigneau 2004), but for caridean shrimp species only the aesthetasc external morphology is described (Table 2; Bauer 1977; Hallberg et al. 1992; Mead 1998; Obermeier and Schmitz 2004; Zhang et al. 2008; Zhu et al. 2011; Solari et al. 2017; Zbinden et al. 2017) and no information is available on the ultrastructure. Aims of the present approach were to investigate potential specificities of the hydrothermal shrimp chemosensory system regarding the aesthetasc cuticle structure and innervation, as well as to provide observations on shrimp aesthetasc ultrastructure to enhance the general knowledge on decapods olfactory systems diversity.

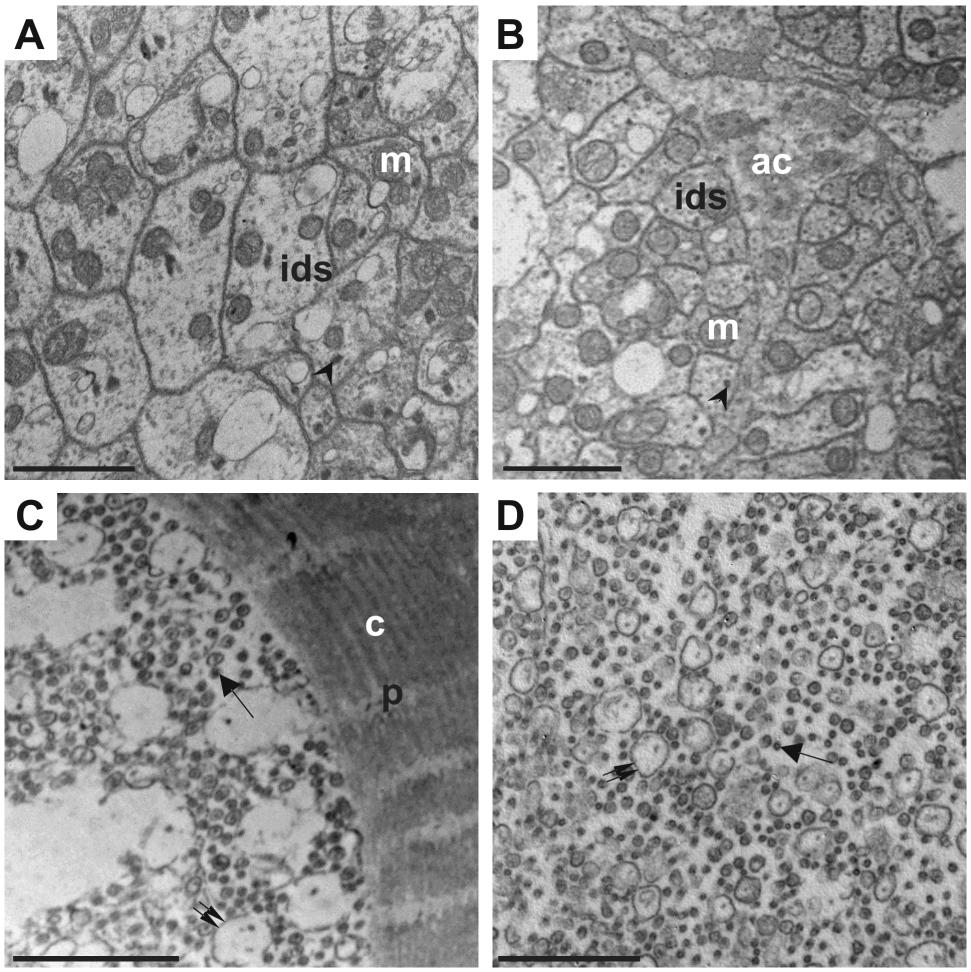

Figure 6. Inner and outer dendritic segments of aesthetasc sensilla of *Mirocaris fortunata* (A, C) and *Palaemon elegans* (B, D). Cross sections through the base (A, B) and the middle (C, D) region of the aesthetasc, showing the inner and outer dendritic segments, respectively. Cuticle (c); auxiliary cell (ac); inner dendritic segment (ids); mitochondrion (m); outer dendritic segment (arrow); pore-like structure (p); ciliary rootlet (arrow head); swelling of dendritic membrane (double arrows). Scale bar = 1 µm.

Aesthetascs of marine decapods are characterized by a thin (0.4–2.1 µm thick, Table 2), poreless cuticle, unlike bimodal sensilla that have a pore at their tip (Garm et al. 2003) and a thick cuticle (e.g., from 2 to 7 µm thick for the distal part of an antennular bimodal sensilla in *R. exoculata*; Machon, personal communication). The aesthetasc cuticle looks spongy, especially in the distal part, possibly functioning as a molecular sieve through which appropriate odorants move quickly to activate OSNs, as reported in spiny lobster (Derby et al. 1997) and crayfish (Tierney et al. 1986). Therefore, the cuticle thickness and structure along the aesthetasc may define the portion of sensilla permeable to soluble odorants. Comparison of aesthetascs from *M. fortunata* and *P. elegans*, and other marine decapod species, reveals similarities in cuticle thickness in the basal region of aesthetascs among the caridean shrimp group, marine crabs and the hermit crab (Table 2), and also in structure, being lamellar (Ghiradella et al. 1968; Grünert and Ache 1988; Gleeson et al. 1996). In our study, the distal region of aesthetascs has a thinner cuticle than described for other decapod species (Table 2), but similar to the thickness of *Daphnia* aesthetasc cuticle (Hallberg et al. 1992), and identical between *M. fortunata* and *P. elegans*. Regarding the cuticle, the spongy nonlamellar cuticle most likely corresponds to the odorant-permeable region. A portion of 50 and 80% of the aesthetasc length has a thin and spongy cuticle in *M. fortunata* and *P. elegans*, respectively. Although the 2 species have a similar aesthetasc length (Zbinden et al. 2017), *P. elegans* aesthetascs appear to have a larger surface area permeable to odorants than *M. fortunata*, which could lead to better sampling of the environment and spatial resolution.

Pore-like structures occur in the aesthetasc cuticle of *M. fortunata* from and beyond the transitional zone, but are absent in the thin cuticle of the distal part of the aesthetasc. These structures and pattern were also found in the hydrothermal shrimp *R. exoculata*, but not in the coastal shrimp *P. elegans*. Other types of pore-like structures have been described in the basal region of the aesthetasc for some marine decapods. Pore canals perforate the lamellar cuticle of the basal tenth of the aesthetascs in the hermit crab *Pagurus hirsutiusculus* (Ghiradella et al. 1968), proximal to the ciliary segments of the transitional zone, and pore-like structures occur from the base to the transitional zone in the lobster *Panulirus argus*, and contain extensions of the auxiliary cells (Grünert and Ache 1988). However, in *M. fortunata* these pore-like structures appear only from and beyond the transitional zone, where the auxiliary cells end. In addition these pore-like structures are much more abundant than those described in *P. hirsutiusculus* and *P. argus*, and are longer, crossing almost the entire thickness of the

cuticle, making them likely a feature specific to hydrothermal shrimp. The function of these pore-like structures is unknown. Although the cuticle layer separating the inner side of the pore-like structures with the outside is extremely thin, they could facilitate the passage of odorant molecules through the thick lamellar cuticle and thus enhance the sampling of the environment by compensating the small surface permeable to odorants in *M. fortunata* aesthetascs.

The presence of a thick layer of bacteria covering the aesthetascs is also likely a feature specific to hydrothermal shrimp. Indeed, dense bacterial populations have been observed on the antennae and antennules of 4 hydrothermal shrimp species (Zbinden et al. 2017; Figure 6C,E,F), sometimes covering the major surface of the aesthetascs, whereas no bacterial coverage was ever observed with the coastal shrimp *P. elegans*. Identification of the different bacteria types present on each species is needed to discuss on their potential role or impact on shrimp sensory perception.

Increased IDSs and ODSs numbers could be associated to a better discrimination of the chemical environment (Derby and Weissburg 2014) because the OSNs (whose number is reflected by the number of IDSs) express different olfactory receptors, beared by the ODSs. The number of IDSs per aesthetasc for *M. fortunata* and *P. elegans* fits within the range of about 100–400 displayed by several Malacostracan taxons (Table 2; Harzsch and Krieger 2018). Compared to *P. elegans*, aesthetascs of *M. fortunata* house fewer OSNs and contain fewer ODSs, suggesting the hydrothermal species is not likely to have an enhanced chemosensitivity regarding this character. However, these data need to be completed by identifying and quantifying the receptor proteins expressed by OSNs for each species, to investigate potential adaptations of the hydrothermal species at the molecular level.

Conclusions and perspectives

This study presents the first insights into the detection of various organic and chemical compounds by hydrothermal shrimp using an EAG approach. Sulfide was detected by both the antennule and the antenna, suggesting that hydrothermal shrimp may be able to sense sulfide concentrations occurring naturally in the near field of the vents. However, this detection is not specific to hydrothermal species. Neurons responding to sulfide are presumably present at least in Palaemonidae and Alvinocarididae shrimp groups, but the behavioral responses triggered by this detection remains unknown. Sulfide is a good candidate as a short-distance orientation cue in hydrothermal environments, as well as food-related odors, and behavioral designs are being experimented to see whether *M. fortunata* use these chemical sources for orientation around vent chimneys. In contrast, manganese and iron did not trigger significant EAG responses, which puts in doubt the significance of chemoreception for long-distance detection of active vents. Chemoreception abilities of other life stages should also be investigated, because dispersal and colonization processes occur at the larval stage (Lutz et al. 1984), which may be more sensitive to long-distance stimuli than adults. Furthermore, behavioral responses to both short- and long-distance stimuli must be investigated for *M. fortunata* and other hydrothermal species using pressurized aquaria (Shillito et al. 2014). Shrimp species occupy distinct microhabitats around vent chimneys, thus may not be sensitive to the same attractants and could exhibit different chemosensory abilities.

Comparative description of the aesthetasc ultrastructure gave insights into features of the hydrothermal shrimp, including cuticular pore-like structures and large bacteria covering. Bacterial functional types are being identified by sequencing approaches to ultimately discuss their potential influence on vent shrimp chemosensory abilities. Examination of the aesthetasc cuticle thickness and the numbers of IDSs and ODSs innervating aesthetascs did not reveal noticeable specializations of the hydrothermal species. Molecular studies are being conducted to further investigate adaptations of hydrothermal species by identifying, quantifying and localizing the chemoreceptors expressed by OSNs.

Funding

This work was supported in part by Sorbonne Université, UPMC and by the European Union Seventh Framework Programme (FP7/2007–2013) under the MIDAS project [grant agreement n°603418].

Acknowledgements

We thank the chief scientists of the Momarsat 2011, 2012, and 2016 cruises (Mathilde Cannat and Pierre-Marie Sarradin), and the chief scientist of the Biobaz 2013 cruise (François Lallier). We also thank Jozée Sarrazin and Nicolas Rabet for hydrothermal and coastal shrimp sampling, respectively, and Cécile Konn for her help with the preparation of chemical stimuli. TEM was performed at the "Plateforme de Microscopie Electronique" (MNHN) with the help of Chakib Djediat.

Conflict of interest

We have no conflict of interest to declare.

References

Ache BW. 1982. Chemoreception and thermoreception. In: Bliss D, editor. *The biology of Crustacea,* Vol. 3. New York: Academic Press. p. 369–398.

Ache BW, Derby CD. 1985. Functional organization of olfaction in crustaceans. *Trends Neurosci.* 8:356–360.

Altner H, Prillinger L. 1980. Ultrastructure of invertebrate chemo-, thermo-, and hygroreceptors and its functional significance. *Int Rev Cytol.* 67:69–139.

Aumond V. 2013. *Spéciation du cuivre en milieu hydrothermal profond et dans les zones de suintements froids* [dissertation]. Université de Bretagne occidentale-Brest.

Baker ET, Resing JA, Haymon RM, Tunnicliffe V, Lavelle JW, Martinez F, Ferrini V, Walker SL, Nakamura K. 2016. How many vent fields? New estimates of vent field populations on ocean ridges from precise mapping of hydrothermal discharge locations. *Earth Planet Sci Lett.* 449:186–196.

Bargmann CI. 2006. Comparative chemosensation from receptors to ecology. *Nature*. 444:295–301.

Bauer RT. 1977. Antifouling adaptations of marine shrimp (Crustacea: Decapoda: Caridea): functional morphology and adaptive significance of antennular preening by the third maxillipeds. *Mar Biol*. 40:261–276.

Beltz BS, Kordas K, Lee MM, Long JB, Benton JL, Sandeman DC. 2003. Ecological, evolutionary, and functional correlates of sensilla number and glomerular density in the olfactory system of decapod crustaceans. *J Comp Neurol*. 455:260–269.

Blaustein DN, Simmons RB, Burgess MF, Derby CD, Nishikawa M, Olson KS. 1993. Ultrastructural localization of 5'AMP odorant receptor sites on the dendrites of olfactory receptor neurons of the spiny lobster. *J Neurosci*. 13:2821–2828.

Carr WE, Ache BW, Gleeson RA. 1987. Chemoreceptors of crustaceans: similarities to receptors for neuroactive substances in internal tissues. *Environ Health Perspect*. 71:31–46.

Casanova B, Brunet M, Segonzac M. 1993. L'impact d'une épibiose bactérienne sur la morphologie fonctionnelle de crevettes associées à l'hydrothermalisme médio-Atlantique. *Cah Biol Mar*. 34:573–588.

Cate HS, Derby CD. 2001. Morphology and distribution of setae on the antennules of the Caribbean spiny lobster *Panulirus argus* reveal new types of bimodal chemo-mechanosensilla. *Cell Tissue Res*. 304:439–454.

Chamberlain SC. 2000. Vision in hydrothermal vent shrimp. *Philos Trans R Soc Lond B Biol Sci*. 355:1151–1154.

Charlou JL, Donval JP, Douville E, Jean-Baptiste P, Radford-Knoery J, Fouquet Y, Dapoigny A, Stievenard M. 2000. Compared geochemical signatures and the evolution of Menez Gwen (37°50′ N) and Lucky Strike (37°17′ N) hydrothermal fluids, south of the Azores Triple Junction on the Mid-Atlantic Ridge. *Chem Geol*. 171:49–75.

Colaço A, Dehairs F, Desbruyères D. 2002. Nutritional relations of deep-sea hydrothermal fields at the Mid-Atlantic Ridge: a stable isotope approach. *Deep Sea Res I*. 49:395–412.

Cottin D, Shillito B, Chertemps T, Thatje S, Léger N, Ravaux J. 2010. Comparison of heat-shock responses between the hydrothermal vent shrimp *Rimicaris exoculata* and the related coastal shrimp *Palaemonetes varians*. *J Exp Marine Biol Ecol*. 393:9–16.

Cowen JP, Massoth GJ, Feely RA. 1990. Scavenging rates of dissolved manganese in a hydrothermal vent plume. *Deep Sea Res I*. 37:1619–1637.

Crone TJ, Wilcock WS, Barclay AH, Parsons JD. 2006. The sound generated by mid-ocean ridge black smoker hydrothermal vents. *PLoS One*. 1:e133.

Cuvelier D, Sarradin PM, Sarrazin J, Colaço A, Copley TJ, Desbruyères D, Glover AG, Santos RS, Tyler PA. 2011. Hydrothermal faunal assemblages and habitat characterization at the Eiffel Tower edifice (Lucky Strike, Mid-Atlantic Ridge). *Mar Ecol*. 32:243–255.

De Angelis MA, Lilley MD, Baross JA. 1993. Methane oxidation in deep-sea hydrothermal plumes of the endeavour segment of the Juan de Fuca Ridge. *Deep Sea Res I*. 40:1169–1186.

De Busserolles F, Sarrazin J, Gauthier O, Gélinas Y, Fabri MC, Sarradin PM, Desbruyères D. 2009. Are spatial variations in the diets of hydrothermal fauna linked to local environmental conditions? *Deep Sea Res II*. 56:1649–1664.

Derby CD. 1982. Structure and function of cuticular sensilla of the lobster *Homarus americanus*. *J Crustac Biol*. 2:1–21.

Derby CD. 1995. Single unit electrophysiological recordings from crustacean chemoreceptor neurons. In: Spielman AI, Brand JG, editors. *Experimental cell biology of taste and olfaction: current techniques and protocols*. Boca Raton (FL): CRC Press. p. 241–250.

Derby CD, Cate HS, Gentilcore LR. 1997. Perireception in olfaction: molecular mass sieving by aesthetasc sensillar cuticle determines odorant access to receptor sites in the Caribbean spiny lobster *Panulirus argus*. *J Exp Biol*. 200:2073–2081.

Derby CD, Kozma MT, Senatore A, Schmidt M. 2016. Molecular mechanisms of reception and perireception in crustacean chemoreception: a comparative review. *Chem Senses*. 41:381–398.

Derby CD, Weissburg MJ. 2014. The chemical senses and chemosensory ecology of crustaceans. In: Derby CD, Thiel M, editors. *Crustacean nervous systems and their control of behavior*. New York: Springer. p. 263–293.

Desbruyères D, Almeida A, Biscoito M, Comtet T, Khripounoff A, Le Bris N, Sarradin PM, Segonzac M. 2000. A review of the distribution of hydrothermal vent communities along the northern Mid-Atlantic Ridge: dispersal vs. environmental controls. *Hydrobiologia*. 440:201–216.

Desbruyères D, Biscoito M, Caprais JC, Colaço A, Comtet T, Crassous P, Fouquet Y, Khripounoff A, Le Bris N, Olu K, *et al.* 2001. Variations in deep-sea hydrothermal vent communities on the Mid-Atlantic Ridge near the Azores plateau. *Deep Sea Res II*. 48:1325–1346.

Doolin RE, Zhainazarov AB, Ache BW. 2001. An odorant-suppressed Cl- conductance in lobster olfactory receptor cells. *J Comp Physiol A*. 187:477–487.

Fuzessery ZM, Childress JJ. 1975. Comparative chemosensitivity to amino acids and their role in the feeding activity of bathypelagic and littoral crustaceans. *Biol Bull*. 149:522–538.

Garm A, Hallberg E, Høeg JT. 2003. Role of maxilla 2 and its setae during feeding in the shrimp *Palaemon adspersus* (Crustacea: Decapoda). *Biol Bull*. 204:126–137.

Garm A, Walting K. 2013. The crustacean integument: setae, setules, and other ornamentation. *Funct Morphol Divers*. 1:167–198.

Gaten E, Herring PJ, Shelton PMJ, Johnson ML. 1998. Comparative morphology of the eyes of postlarval bresiliid shrimps from the region of hydrothermal vents. *Biol Bull*. 194:267–280.

Gebruk AV, Southward EC, Kennedy H, Southward AJ. 2000. Food sources, behaviour, and distribution of hydrothermal vent shrimps at the Mid-Atlantic Ridge. *J Mar Biol Assoc UK*. 80:485–499.

Ghiradella HT, Case JF, Cronshaw J. 1968. Structure of aesthetases in selected marine and terrestrial decapods: chemoreceptor morphology and environment. *Am Zool*. 8:603–621.

Gleeson RA, McDowell LM, Aldrich HC. 1996. Structure of the aesthetasc (olfactory) sensilla of the blue crab, *Callinectes sapidus*: transformations as a function of salinity. *Cell Tissue Res*. 284:279–288.

Grünert U, Ache BW. 1988. Ultrastructure of the aesthetasc (olfactory) sensilla of the spiny lobster, *Panulirus argus*. *Cell Tissue Res*. 251:95–103.

Hallberg E, Chaigneau J. 2004. Non-visual sense organs. In: Forest J, von Vaupel Klein JC, editors. *Treatise on zoology, Crustacea,* Vol. 1. Leiden (NL): Brill Academic Publishers. p. 301–380.

Hallberg E, Johansson KU, Elofsson R. 1992. The aesthetasc concept: structural variations of putative olfactory receptor cell complexes in Crustacea. *Microsc Res Tech*. 22:325–335.

Hallberg E, Skog M. 2010. Chemosensory sensilla in crustaceans. In: Breithaupt T, Thiel M, editors. *Chemical communication in crustaceans*. New York: Springer. p. 103–121.

Hamilton KA, Ache BW. 1983. Olfactory excitation of interneurons in the brain of the spiny lobster. *J Comp Physiol*. 150:129–140.

Harzsch S, Krieger J. 2018. Crustacean olfactory systems: a comparative review and a crustacean perspective on insect olfactory systems. *Prog Neurobiol*. 161:23–60.

Hernández-Ávila I, Cambon-Bonavita MA, Pradillon F. 2015. Morphology of first zoeal stage of four genera of alvinocaridid shrimps from hydrothermal vents and cold seeps: implications for ecology, larval biology and phylogeny. *PLoS One*. 10:e0144657.

Herring PJ, Dixon DR. 1998. Extensive deep-sea dispersal of postlarval shrimp from a hydrothermal vent. *Deep Sea Res I*. 45:2105–2118.

Hourdez S, Lallier FH. 2007. Adaptations to hypoxia in hydrothermal-vent and cold-seep invertebrates. *Rev Environ Sci Biotechnol*. 6:143–159.

Jinks RN, Battelle BA, Herzog ED, Kass L, Renninger GH, Chamberlain SC. 1998. Sensory adaptations in hydrothermal vent shrimps from the Mid-Atlantic Ridge. *Cah Biol Mar*. 39: 309–312.

Klevenz V, Bach W, Schmidt K, Hentscher M, Koschinsky A, Petersen S. 2011. Geochemistry of vent fluid particles formed during initial hydrothermal fluid-seawater mixing along the Mid-Atlantic Ridge. *Geochem Geophys Geosyst*. 12:Q0AE05. doi:10.1029/2011GC003704.

Lagerspetz KY, Vainio LA. 2006. Thermal behaviour of crustaceans. *Biol Rev Camb Philos Soc*. 81:237–258.

Lallier FH, Truchot JP. 1997. Hemocyanin oxygen-binding properties of a deep-sea hydrothermal vent shrimp: evidence for a novel cofactor. *J Exp Zool*. 277:357–364.

Laverack MS. 1964. The antennular sense organs of *Panulirus argus*. *Comp Biochem Physiol*. 13:301–321.

Laverack MS. 1988. The diversity of chemoreceptors. In: Atema J, Fay RR, Tavolga WN, editors. *Sensory biology of aquatic animals*, Vol. 3. New York: Springer-Verlag. p. 287–312.

Laverack MS, Ardill DJ. 1965. The innervation of the aesthetasc hairs of *Panulirus argus*. *J Cell Sci.* 3:45–60.

Le Bris N, Govenar B, Le Gall C, Fisher CR. 2006. Variability of physicochemical conditions in 9°50′ N EPR diffuse flow vent habitats. *Mar Chem*. 98:167–182.

Lutz RA, Jablonski D, Turner RD. 1984. Larval development and dispersal at deep-sea hydrothermal vents. *Science*. 226:1451–1454.

Machon J, Ravaux J, Zbinden M, Lucas P. 2016. New electroantennography method on a marine shrimp in water. *J Exp Biol*. 219:3696–3700.

Martin JW, Christiansen JC. 1995. A new species of the shrimp genus *Chorocaris* Martin & Hessler, 1990 (Crustacea: Decapoda: Bresiliidae) from hydrothermal vent fields along Mid-Atlantic Ridge. *Proc Biol Soc Wash*. 108:220–227.

Martin JW, Haney TA. 2005. Decapod crustaceans from hydrothermal vents and cold seeps: a review through 2005. *Zool J Linn Soc*. 145:445–522.

Matabos M, Cuvelier D, Brouard J, Shillito B, Ravaux J, Zbinden M, Barthelemy D, Sarradin PM, Sarrazin J. 2015. Behavioural study of two hydrothermal crustacean decapods: *Mirocaris fortunata* and *Segonzacia*

mesatlantica, from the Lucky Strike vent field (Mid-Atlantic Ridge). *Deep Sea Res II*. 121:146–158.

Mead KS. 1998. The biomechanics of odorant access to aesthetascs in the grass shrimp, *Palaemonetes vulgaris*. *Biol Bull*. 195:184–185.

Mellon D Jr. 2000. Convergence of multimodal sensory input onto higher-level neurons of the crayfish olfactory pathway. *J Neurophysiol*. 84:3043–3055.

Monteclaro HM, Anraku K, Matsuoka T. 2010. Response properties of crayfish antennules to hydrodynamic stimuli: functional differences in the lateral and medial flagella. *J Exp Biol*. 213:3683–3691.

Mottl MJ, McConachy TF. 1990. Chemical processes in buoyant hydrothermal plumes on the East Pacific Rise near 21°N. *Geochim Cosmochim Acta*. 54:1911–1927.

Nagai T. 1985. Summation and gradient characteristics of local electroantennogram response of the European corn borer, *Ostrinia nubilalis*. *Pestic Biochem Physiol*. 24:32–39.

Obermeier M, Schmitz B. 2004. The modality of the dominance signal in snapping shrimp (*Alpheus heterochaelis*) and the corresponding setal types on the antennules. *Mar Freshwater Behav Physiol*. 37:109–126.

Pelli DG, Chamberlin SC. 1989. The visibility of 350 degrees C black-body radiation by the shrimp *Rimicaris exoculata* and man. *Nature*. 337:460–461.

Polz MF, Robinson JJ, Cavanaugh CM, Van Dover CL. 1998. Trophic ecology of massive shrimp aggregations at a Mid-Atlantic Ridge hydrothermal vent site. *Limnol Oceanogr*. 43:1631–1638.

Ponsard J, Cambon-Bonavita MA, Zbinden M, Lepoint G, Joassin A, Corbari L, Shillito B, Durand L, Cueff-Gauchard V, Compère P. 2013. Inorganic carbon fixation by chemosynthetic ectosymbionts and nutritional transfers to the hydrothermal vent host-shrimp *Rimicaris exoculata*. *ISME J*. 7:96–109.

Puri S, Faulkes Z. 2010. Do decapod crustaceans have nociceptors for extreme pH? *PLoS One*. 5:e10244.

Radford-Knoery J, Charlou JL, Donval JP, Aballea M, Fouquet Y, Ondreas H. 1998. Distribution of dissolved sulfide, methane, and manganese near the seafloor at the Lucky Strike (37°17′N) and Menez Gwen (37°50′N) hydrothermal vent sites on the mid-Atlantic Ridge. *Deep Sea Res I*. 45:367–386.

Rathke H. 1837. Zur Fauna der Krym. *Mémoires de l'Académie Impériale des Sciences de St. Pétersbourg*. 3:291–454.

Ravaux J, Cottin D, Chertemps T, Hamel G, Shillito B. 2009. Hydrothermal vent shrimps display low expression of the heat-inducible hsp70 gene in nature. *Mar Ecol Prog Ser*. 396:153–156.

Renninger GH, Kass L, Gleeson RA, Van Dover CL, Battelle BA, Jinks RN, Herzog ED, Chamberlain SC. 1995. Sulfide as a chemical stimulus for deep-sea hydrothermal vent shrimp. *Biol Bull*. 189:69–76.

Rospars JP, Grémiaux A, Jarriault D, Chaffiol A, Monsempes C, Deisig N, Anton S, Lucas P, Martinez D. 2014. Heterogeneity and convergence of olfactory first-order neurons account for the high speed and sensitivity of second-order neurons. *PLoS Comput Biol*. 10:e1003975.

Sarradin PM, Caprais JC, Riso R, Kerouel R, Aminot A. 1999. Chemical environment of the hydrothermal mussel communities in the lucky strike and Menez Gwen vent fields, Mid Atlantic Ridge. *Cah Biol Mar*. 40:93–104.

Sarrazin J, Juniper SK, Massoth G, Legendre P. 1999. Physical and chemical factors influencing species distributions on hydrothermal sulfide edifices of the Juan de Fuca Ridge, northeast Pacific. *Mar Ecol Prog Ser*. 190:89–112.

Sarrazin J, Legendre P, De Busserolles F, Fabri MC, Guilini K, Ivanenko VN, Morineaux M, Vanreusel A, Sarradin PM. 2015. Biodiversity patterns, environmental drivers and indicator species on a high-temperature hydrothermal edifice, Mid-Atlantic Ridge. *Deep Sea Res II*. 121:177–192.

Sarrazin J, Sarradin PM, Allais AG. 2006. MoMARETO: a cruise dedicated to the spatio-temporal dynamics and the adaptations of hydrothermal vent fauna on the Mid-Atlantic Ridge. *InterRidge News*. 15:24–33.

Schmidt M, Ache BW. 1996. Processing of antennular input in the brain of the spiny lobster, *Panulirus argus*. *J Comp Phys A*. 178:605–628.

Schmidt M, Mellon F. 2010. Neuronal processing of chemical information in crustaceans. In: Breithaupt T, Thiel M, editors. *Chemical communication in crustaceans*. New York: Springer. p. 123–147.

Shillito B, Gaill F, Ravaux J. 2014. The IPOCAMP pressure incubator for deep-sea fauna. *J Mar Sci Tech*. 22:97–102.

Shillito B, Hamel G, Duchi C, Cottin D, Sarrazin J, Sarradin PM, Ravaux J, Gaill F. 2008. Live capture of megafauna from 2300 m depth, using a newly designed pressurized recovery device. *Deep Sea Res I*. 55:881–889.

Shillito B, Ravaux J, Sarrazin J, Zbinden M, Sarradin PM, Barthelemy D. 2015. Long-term maintenance and public exhibition of deep-sea hydrothermal fauna: the AbyssBox project. *Deep Sea Res II*. 121:137–145.

Snow PJ. 1973. Ultrastructure of the aesthetase hairs of the littoral decapod, *Paragrapsus gaimardii*. *Z Zellforsch Mikrosk Anat*. 138:489–502.

Solari P, Sollai G, Masala C, Loy F, Palmas F, Sabatini A, Crnjar R. 2017. Antennular morphology and contribution of aesthetascs in the detection of food-related compounds in the shrimp *Palaemon adspersus* Rathke, 1837 (Decapoda: Palaemonidae). *Biol Bull*. 232:110–122.

Spencer M, Linberg KA. 1986. Ultrastructure of aesthetasc innervation and external morphology of the lateral antennule setae of the spiny lobster *Panulirus interruptus* (Randall). *Cell Tissue Res*. 245:69–80.

Tierney AJ, Thompson CS, Dunham DW. 1986. Fine structure of aesthetasc chemoreceptors in the crayfish *Orconectes propinquus*. *Can J Zool*. 64:392–399.

Toner BM, Santelli CM, Marcus MA, Wirth R, Chan CS, McCollom T, Bach W, Edwards KJ. 2009. Biogenic iron oxyhydroxide formation at mid-ocean ridge hydrothermal vents: Juan de Fuca Ridge. *Geochim Cosmochim Acta*. 73:388–403.

Tyler PA, Young CM. 2003. Dispersal at hydrothermal vents: a summary of recent progress. *Hydrobiologia*. 503:9–19.

Ukhanov K, Bobkov Y, Ache BW. 2011. Imaging ensemble activity in arthropod olfactory receptor neurons *in situ*. *Cell Calcium*. 49:100–107.

Van Dover CL, Szuts EZ, Chamberlain SC, Cann JR. 1989. A novel eye in 'eyeless' shrimp from hydrothermal vents of the Mid-Atlantic Ridge. *Nature*. 337:458–460.

van Drongelen W, Holley A, Døving KB. 1978. Convergence in the olfactory system: quantitative aspects of odour sensitivity. *J Theor Biol*. 71:39–48.

Waeles M, Cotte L, PErnet-Coudrier B, Chavagnac V, Cathalot C, Leleu T, Laës-Huon A, Perhirin A, Riso RD, Sarradin PM. 2017. On the early fate on hydrothermal iron at deep-sea vents: a reassessment after in situ filtration. *Geophys Res Let*. 44:4233–4240.

Zbinden M, Berthod C, Montagné N, Machon J, Léger N, Chertemps T, Rabet N, Shillito B, Ravaux J. 2017. Comparative study of chemosensory organs of shrimp from hydrothermal vent and coastal environments. *Chem Senses*. 42:319–331.

Zbinden M, Shillito B, Le Bris N, de Montlaur CDV, Roussel E, Guyot F, Gaill F, Cambon-Bonavita MA. 2008. New insights on the metabolic diversity among the epibiotic microbial community of the hydrothermal shrimp *Rimicaris exoculata*. *J Exp Mar Biol Ecol*. 359:131–140.

Zhang D, Cai S, Liu H, Lin J. 2008. Antennal sensilla in the genus *Lysmata* (Caridea). *J Crustac Biol*. 28:433–438.

Zhang JZ, Millero FJ. 1993. The products from the oxidation of H_2S in seawater. *Geochim Cosmochim Acta*. 57:1705–1718.

Zhu J, Zhang D, Lin J. 2011. Morphology and distribution of antennal and antennular setae in *Lysmata* shrimp. *J Shellfish Res*. 30:381–388.